Geological Society of America
Special Paper 247
1990

Asteroid and comet flux in the neighborhood of Earth

Eugene M. Shoemaker, Ruth F. Wolfe, and Carolyn S. Shoemaker
U.S. Geological Survey, 2255 North Gemini Drive, Flagstaff, Arizona 86001

ABSTRACT

Approximately 90 Earth-crossing asteroids had been discovered through September 1989. Discovery is thought to be complete at absolute V magnitude (H) = 13.2 (the magnitude of the brightest known object, diameter ~8.1 km), and about 6 percent complete at H = 17.7 (typical diameter about 1 km). The calculated mean probability of collision of Earth-crossing asteroids with Earth is $(4.2 \pm 1.7) \times 10^{-9}$ yr^{-1}. When multiplied by the estimated population of 1030 ± 470 at H = 17.7, this probability yields a collision rate of $(4.3 \pm 2.6) \times 10^{-6}$ yr^{-1} for asteroids larger than about 1 km in diameter. At H = 15.8, roughly equivalent to asteroid diameters more than 2 km, the estimated collision rate is $\approx 7 \times 10^{-7}$ yr^{-1}, and at 8-km diameter, the rate is $\approx 3 \times 10^{-9}$ yr^{-1}. Comet nuclei with diameters more than 2.5 km are estimated to strike the Earth at the rate of $\approx 10^{-7}$ yr^{-1}; comets larger than 10 km in diameter probably strike at a rate $\approx 10^{-8}$ yr^{-1}. Impact of asteroids probably dominates the production of craters smaller than 30 km in diameter, whereas comet impact probably forms most craters larger than 50 km. The production rate for craters larger than 20 km in diameter, estimated from the astronomical evidence, is $(4.9 \pm 2.9) \times 10^{-15}$ km^{-2} yr^{-1}; this rate is consistent with the cratering rate estimated by Grieve from the geologic record for the last 120 m.y.

INTRODUCTION

Significant advances in our knowledge and understanding of the flux of large, solid objects in the neighborhood of Earth have occurred since the last Snowbird Conference in 1981. We present here our best estimates of the collision rates with Earth of asteroids and comets and the corresponding production of impact craters.

Approximately 90 Earth-crossing asteroids had been discovered through September 1989 (Table 1). Of these objects, 59 have precisely determined orbits and are numbered, ten are lost, and most of the remainder have been discovered too recently to have been observed on a second apparition. The mean rate of discovery increased to seven per year from 1986 through the first nine months of 1989, about double the previous ten-year average. As shown by this high rate, the discovery of Earth crossers is far from complete.

The term Earth-crossing asteroid is used here, following the definition of Shoemaker and others (1979), to denote an asteroid whose orbit can intersect the orbit of Earth as a result of secular (long-range) perturbations by the planets. For asteroids revolving on orbits that overlap Earth's, intersections (crossings) occur chiefly as a consequence of precession of the major axis of each asteroid's orbit. In a full cycle of precession, the distance from the Sun to each node (the points of intersection of the asteroid's orbit on the orbit plane of the Earth), here called the radius to the node, oscillates between the perihelion and aphelion distances (the distances from the Sun to the near and far extremities of the major axis). Crossing occurs when one of the two nodes coincides with the Earth's orbit. If the orbits of the asteroid and of Earth overlap continuously, four crossings take place during one cycle of advance of the perihelion. Precession periods for Earth-crossing asteroids range from approximately 4,000 to 100,000 years (Table 1); a fast precessor crosses as frequently as about once per 1,000 years.

Three categories of Earth-crossing asteroids generally are recognized (Shoemaker and others, 1979); Atens, Apollos, and Amors. Aten asteroids have orbits smaller than Earth's and overlap Earth's orbit in the region of their aphelia. Apollo asteroids have orbits larger than Earth's and overlap near their perihelia. Earth-crossing Amor asteroids have orbits larger than Earth's and can approach the Earth, but their current perihelion distances are

Shoemaker, E. M., Wolfe, R. F., and Shoemaker, C. S., 1990, Asteroid and comet flux in the neighborhood of Earth, *in* Sharpton, V. L., and Ward, P. D., eds., Global catastrophes in Earth history; An interdisciplinary conference on impacts, volcanism, and mass mortality: Geological Society of America Special Paper 247.

TABLE 1. EARTH-CROSSING ASTEROIDS: MAGNITUDES, DIAMETERS, CROSSING DEPTHS, AND COLLISION PARAMETERS

		H	Diam km	Depth AU	a AU	e	i deg	dr/dt $\frac{AU}{10^4 yr}$	Tc 10^4yr	Ps $\frac{1}{10^9 yr}$	Po $\frac{1}{10^9 yr}$	vi km/s
ATEN ASTEROIDS												
2340	Hathor	20.2	(0.2)	0.356	0.844	0.424	6.27	0.28	9.54	14	14	16.3
2100	Ra-Shalom	16.12	2.4	0.388	0.832	0.465	13.1	0.32	9.91	6.3	6.7	17.9
3753	1986 TO	15.0	~3	.....	0.998	(0.50)	(22)	.....	.....	.....	(3)	(22)
	1954 XA (L)	18.9	~0.5	0.203	0.777	0.389	5.04	0.14	10.9	34	30	14.5
3362	Khufu	18.15	0.7	0.559	0.990	0.514	8.37	0.61	7.36	5.3	6.2	19.8
2062	Aten	16.96	0.9	0.223	0.966	0.231	18.0	0.19	7.09	7.1	6.5	16.0
3554	Amun	15.94	2.0	0.299	0.974	0.251	21.6	0.14	10.5	5.4	5.0	17.4
APOLLO ASTEROIDS												
3200	Phaethon	14.65	6.9	.....	1.271	(0.89)	(22)	.....	.....	.....	(1.4)	(35)
1566	Icarus	16.45	0.9	0.844	1.078	0.810	18.0	2.0	5.33	1.8	2.2	30.6
2212	Hephaistos	14.0	~5	0.929	2.163	0.889	10.0	32	0.83	0.44	1.2	34.6
	1974 MA (L)	14.0	~5	.....	1.757	0.446	53.4	0.66	4.23	0.93	2.5	32.0
						0.772	32.8	3.6				
	1984 KB	16.4	1.4	0.760	2.221	0.807	3.37	24	0.76	1.1	3.2	28.8
	5025 P-L (L)	15.9	~2	.....	(4.2)	(0.90)	(6.2)	.....	.....	.....	(~1)	(32)
1864	Daedalus	15.02	(3.1)	0.491	1.461	0.640	15.9	2.1	3.69	1.0	1.6	26
3838	1986 WA	15.5	~3	.....	1.505	(0.70)	(29)	.....	.....	.....	(1)	(29)
2201	Oljato	15.56	1.4	0.657	2.174	0.765	1.33	16	0.89	2.3	6.1	26.4
2101	Adonis	18.2	~1	0.620	1.875	0.727	2.03	7.1	1.58	2.8	6.2	25.4
1865	Cerberus	16.8	1.0	0.504	1.080	0.513	14.9	0.68	6.81	2.5	3.1	20.9
	1987 SY	17.5	~1	0.523	1.442	0.615	1.88	2.1	3.35	6.3	10.4	22.2
3752	1985 PA	15.6	~2	.....	1.414	(0.61)	(32)	.....	.....	.....	(1)	(27)
	1989 PB	17.2	~1	0.479	1.063	0.466	9.68	0.59	6.986	4.2	5.1	18.9
	1979 XB (L)	19.0	~0.5	(0.56)	2.264	(0.75)	(10.2)	(12)	(1.0)	(0.5)	(1.2)	(25)
	1987 KF	15.5	~3	0.511	1.837	0.676	5.88	4.6	1.84	1.5	2.9	23.3
4034	1986 PA	18.2	~1	0.438	1.060	0.428	10.0	0.49	7.10	4.5	5.3	18.0
3360	1981 VA	16.55	1.8	0.346	2.462	0.611	38.6	1.9	1.49	0.66	1.6	26.6
						0.751	20.8	7.0				
	1937 UB (L)	17.0	~1	0.459	1.639	0.619	5.64	2.6	2.58	2.2	3.7	21.7
1981	Midas	16.9	~1	.....	1.776	0.586	45.5	0.42	2.62	3.8	0.7	30.7
						0.652	41.3	0.53				
	1989 QF	18.0	~1	0.418	1.155	0.447	5.27	0.65	5.88	6.4	8.1	17.9
1862	Apollo	16.23	1.4	0.423	1.471	0.560	6.13	1.5	3.44	2.8	4.3	20.3
	1987 OA	18.5	~1	0.414	1.490	0.570	11.0	1.6	3.50	1.6	2.4	21.1
	1988 EG	18.0	~1	0.399	1.270	0.477	2.71	0.85	4.81	8.8	12	18.3
	1989 FC	20.5	~0.2	0.374	1.024	0.340	4.46	0.36	7.12	13	15	15.4
4183	1959 LM	14.6	~4	0.425	1.981	0.647	7.42	3.9	1.59	1.3	2.2	21.3
1685	Toro	13.92	5.2	.....	1.368	0.438	9.15	0.78	(3)	(4)	(4.2)	17.2
2329	Orthos	15.1	~3	0.295	2.404	0.588	32.6	0.77	1.19	1.8	2.2	23.3
						0.702	16.9	5.2				
2063	Bacchus	17.6	~1	0.330	1.078	0.333	8.99	0.33	7.26	6.5	7.2	15.8
	1989 DA	18.0	~1	0.602	2.166	0.664	5.08	5.6	1.10	1.5	2.8	20.8
	1983 VA	16.5	~2	0.485	2.615	0.718	6.81	17	0.47	0.66	1.6	21.6
	1983 TF2 (L)	17.5	~1	0.413	2.440	0.693	13.9	5.8	0.97	0.53	0.9	22.0
	1989 FB	17.5	~1	0.259	1.044	0.280	13.7	0.31	5.79	6.1	6.0	15.7
	1988 XB	17.0	~1	0.263	1.467	0.469	3.98	1.0	3.11	6.2	7.9	17.0
	1988 TA	21.0	~0.2	0.262	1.541	0.488	3.42	1.1	2.88	6.3	8.2	17.1
	1987 SB	15.5	~3	0.544	2.202	0.645	0.99	4.7	1.03	4.9	8.4	19.3
	1950 DA (L)	15.8	~2	0.266	1.683	0.535	10.7	1.3	2.66	1.9	2.4	18.7
	1978 CA	17.8	1.9	0.293	1.125	0.303	25.5	0.18	8.29	3.6	3.0	19.5
2135	Aristaeus	18.0	~1	.....	1.600	0.490	(23.3)	(0.43)	(3.97)	(2.0)	(1.5)	20.8
	1988 VP4	15.5	~3	0.328	2.263	0.651	10.3	4.0	1.10	0.97	1.5	20.1
1620	Geographos	15.61	2.0	0.210	1.245	0.351	14.2	0.39	5.20	3.8	3.9	16.7
	6743 P-L (L)	17.3	~1	0.245	1.681	0.514	7.55	1.1	2.60	3.0	3.7	17.4
4197	1982 TA	15.4	1.8	.....	2.300	(0.77)	(12)	.....	.....	.....	(1)	(27)
	1973 NA (L)	15.5	~3	.....	2.447	0.672	67.9	2.9	1.47	0.54	0.36	40.5
						0.891	51.8	6.4				
	1989 JA	16.5	~2	0.158	1.769	0.495	14.8	0.54	2.62	2.8	2.3	17.5
	1983 LC	19.0	~0.5	0.334	2.629	0.656	1.54	5.3	0.44	5.8	7.6	16.8

TABLE 1. EARTH-CROSSING ASTEROIDS: MAGNITUDES, DIAMETERS, CROSSING DEPTHS, AND COLLISION PARAMETERS (continued)

		H	Diam km	Depth AU	a AU	e	i deg	dr/dt AU / 10^4yr	Tc 10^4yr	Ps 1 / 10^9yr	Po 1 / 10^9yr	vi km/s
APOLLO ASTEROIDS (continued)												
2102	Tantalus	16.3	~2	.....	1.290	0.312	62.5	0.39	4.87	2.5	1.5	34.8
						0.744	49.1	1.4				
	1989 AZ	19.4	~0.4	0.138	1.649	0.433	9.92	0.36	2.99	5.9	5.0	15.1
	1986 JK	19.0	~1	.....	5:2 commensurability.....			.....	.....	.....	.....	
	1982 DB	18.5	~1	0.093	1.489	0.350	4.88	0.20	3.70	22	20	13.1
4257	1987 QA	16.1	~2	.....	.....	.....	.....	.....	.....	.....	.....	.....
3361	Orpheus	19.9	~0.3	.....	1.209	(0.32)	(2.7)	.....	.....	.....	(21)	(14)
4179	1989 AC	14.2	~4	0.247	2.513	0.609	1.16	0.76	0.66	32	15	14.4
	6344 P-L (L)	21.9	~0.1	0.20	2.619	0.68	3.71	.....	0.56	.....	1.6	18.9
4015	1979 VA	15.5	~5	0.081	2.645	0.639	5.03	.....	0.61	.....	1.0	15
1863	Antinous	15.81	1.8	0.076	2.260	0.579	23.1	.....	1.74	.....	0.54	19.7
3103	1982 BB	15.16	1.5	0.054	1.407	0.308	22.0	.....	5.09	.....	3.8	17.3
3671	Dionysius	17.0	~1	.....	2.198	(0.54)	(14)	.....	.....	.....	(1.5)	(16)
AMOR ASTEROIDS												
2608	Seneca	17.57	0.9	.....	3:1 commensurability.....			.....	.....	.....	.....	
3122	1981 ET3	14.3	~4	0.036	1.768	0.43	19.6	.....	2.98	.....	3.2	16.9
3757	1982 XB	18.69	0.5	0.046	1.838	0.466	2.55	.....	2.35	.....	2.5	13.4
3908	1980 PA	17.7	~1	0.090	1.926	0.513	2.80	.....	1.85	.....	4.0	14.7
	1987 WC	19.5	~0.4	.....	.....	.....	.....	.....	.....	.....	.....	.....
2061	Anza	16.7	(2.7)	0.050	2.263	0.568	3.41	.....	1.24	.....	1.3	14.2
1915	Quetzalcoatl	18.97	0.3	.....	3:1 commensurability.....			.....	.....	.....	.....	
	1980 AA	18.94	(0.5)	0.009	1.892	0.461	3.55	.....	2.10	.....	0.2	13.0
	1987 SF3	19.0	~0.5	0.039	2.25	0.560	3.56	.....	1.28	.....	2.0	13.7
1917	Cuyo	15.2	~3	0.051	2.149	0.545	19.3	.....	1.73	.....	1.3	17.8
1943	Anteros	15.7	1.8	0.024	1.430	0.298	9.35	.....	4.28	.....	1.1	13.4
3988	1986 LA	18.6	~1	-0.002	1.545	0.336	13.4	.....	3.37	.....	.....	.....
3551	1983 RD	16.81	0.9	.....	.....	.....	.....	.....	.....	.....	.....	.....
	1981 QB	16.0	~2	0.064	2.240	0.570	28.5	.....	2.76	.....	0.8	21.7
1221	Amor	18.0	~1	0.061	1.921	0.497	11.9	.....	2.04	.....	1.6	15.4
	1980 WF	18.5	0.6	0.291	2.230	0.670	7.79	.....	1.19	.....	1.0	20.9
	1988 SM	18.0	~1	.....	.....	.....	.....	.....	.....	.....	.....	.....
3288	Seleucus	15.0	2.8	0.319	2.032	0.651	5.46	.....	1.59	.....	1.4	20.8
1580	Betulia	14.55	7.4	.....	2.196	0.564	48.5	1.8	2.37	0.50	1.7	30.6
						0.792	26.4	7.0				
2202	Pele	16.3	~2	0.018	2.291	0.559	8.70	.....	1.27	.....	0.1	14.6
1627	Ivar	13.24	8.1	0.042	1.863	0.471	7.98	.....	2.10	.....	1.8	13.9
	1985 WA	19.0	~0.5	.....	5:2 commensurability.....			.....	.....	.....	.....	
	1987 QB	19.0	~0.5	0.021	2.795	0.640	2.34	.....	0.41	.....	0.1	15.2
887	Alinda	13.79	4.2	.....	3:1 commensurability.....			.....	.....	.....	.....	
	1986 DA	15.94	2.3	.....	5:2 commensurability.....			.....	.....	.....	.....	
	1986 RA	16.0	~4	.....	2:1 commensurability.....			.....	.....	.....	.....	

Aten, Apollo, and Amor asteroids are each listed in order of increasing perihelion distance. Estimated perihelion at the time of Earth-crossing is used to order Atens and Amors. Amors are listed in order of current perihelion distance. Asteroids preceded by a number have precisely determined orbits; those followed by (L) are lost.

H is absolute magnitude in the V band, as determined from observations by internationally adopted formulae (e.g., Batrakov, 1989, p. 8).

The column headed Diam gives the estimated diameter in kilometers. Accurately determined diameters, based on infrared observations, have been taken chiefly from Veeder and others (1989). Diameters estimated from accurate magnitudes, where albedos have been assumed on the basis of spectrophotometric classification, are shown in parentheses. Approximate diameters are listed where magnitudes are based on photographic observations and spectrophotometric class is unknown.

The column headed Depth gives the crossing depth, the maximum overlap of the orbit of the asteroid with the orbit of the Earth along the radius to the node, determined from the theory of Williams (1969).

The orbital elements a (semimajor axis), e (eccentricity), and i (inclination with respect to the invariable plane) and the derivative of the radius to the node, dr/dt, are estimated representative values at the time of Earth-crossing. Tc is the period of precession of the major axis with respect to the line of the nodes in the invariable plane. Ps is the probability of collision with Earth calculated from the equations of Shoemaker and others (1979), and Po is probability of collision with Earth calculated from the equations of Öpik (1951). Uncertain values are shown in parentheses.

The column headed vi gives the impact speed in kilometers per second, corresponding to the orbital elements shown for the time of collision with Earth. Collision is assumed to occur at 1.000 AU, for Atens and deep-crossing Apollos, and at 1.028 AU for shallow-crossing Apollos and Amors.

greater than the aphelion distance of Earth. Secular variation of the eccentricities and, in some cases, of the semimajor axes of Earth-crossing Amors leads to part-time orbital overlap with Earth. Conversely, some Apollos lose overlap and become Amors part of the time. Apollos revolving on certain unusual orbits can lose overlap with Earth before crossings take place because of rapid change in eccentricity during precession. This happens in the case of one known Apollo, 1866 Sisyphus, that at 8.2 km diameter is one of the largest Earth-approaching asteroids. (Because it is not an Earth crosser, Sisyphus does not appear in Table 1.)

A simple test for identification of some but not all Earth crossers is to examine whether the asteroid's orbit is linked with Earth's (i.e., whether one node lies outside Earth's orbit and the other lies inside). All asteroids revolving on orbits that are currently linked with Earth's are crossers. Amors and most Apollos with shallow overlap, on the other hand, can be demonstrated to be Earth crossers only by study of the secular perturbations of their orbits. This study may be done by means either of perturbation theory or of numerical integration of the motion of an asteroid. In some cases, integration of the motion provides the only feasible method of identification. In Table 1, we present the crossing depth (maximum orbital overlap along the radius to the node) for each asteroid whose secular perturbations can be estimated from the theory of Williams (1969). One Amor with a negative crossing depth of 0.002 AU, (3988) 1986 LA, is included as a probable Earth crosser. This asteroid can approach Earth within approximately 300,000 km, about the distance to the Moon; during close approach to Earth the asteroid will be subject to short-range perturbations that can lead to its capture into a crossing orbit.

POPULATION OF EARTH-CROSSING ASTEROIDS

Among 51 new Earth-crossing asteroids found in the last decade, more than two-thirds were discovered from observations at Palomar Observatory; 25 were discovered or independently detected in dedicated surveys with the Palomar 46-cm Schmidt telescope. From the rate of discovery in the Palomar Asteroid and Comet Survey (Shoemaker and Shoemaker, 1988), using the 46-cm Schmidt, and from discoveries made in a prior survey with this instrument (Helin and Shoemaker, 1979), we estimate that the population of Earth crossers brighter than absolute V magnitude (H) = 17.7 (diameter typically about 1 km) is about 1,000. [Note: The symbol H is used here to designate absolute V magnitude as calculated by a formula recently adopted by international agreement (cf. Batrakov, 1987, p. 6); $H \approx V(1,0) - 0.3$, where V(1,0) denotes absolute V magnitude calculated previously on the basis of an assumed linear phase function (cf. Bowell and others, 1979). Absolute V magnitude 17.7 in the new system is approximately equivalent to absolute V magnitude 18.0 in the old system.]

The population has been estimated from the discovery rate by the following approach. Most Earth-crossing asteroids are so small and intrinsically faint that they are only detectable in wide-field telescopes when they are moderately close to the Earth. In our survey with the 46-cm Schmidt, detection is achieved by stereoscopic methods with a pair of photographs, usually taken about 45 minutes apart. Near-Earth asteroids are discriminated by exceptionally fast angular motion or by peculiar direction of motion. For near-Earth objects, each field photographed samples a conical volume of space; the apical angle of this cone is 8°.75, the angular width of the field; the height of the cone is given by the distance to which an asteroid of a given magnitude can be detected by the photographic method and search techniques that we employ. This distance is given by

$$\log \Delta = 0.2\,[V - H - 5\log r - f(\alpha)], \qquad (1)$$

where Δ is distance of the asteroid from Earth in AU, V is apparent V magnitude, r is distance from the Sun, and $f(\alpha)$ is the phase function. The phase angle, α, is the angle between the vectors from the asteroid to the Earth and from the asteroid to the Sun. At a typical threshold of detection of V = 16.5, a distance from the Sun, r, close to $1 + \Delta$, and a mean value of $f(\alpha)$ near 0.8 for the observing strategy of our survey, the height of the conical region sampled for an asteroid with H = 17.7 is 0.3 AU. In principle, brighter (lower H) asteroids can be detected at distances much greater than 0.3 AU, as can be seen from equation (1), but in practice, Earth-crossing asteroids are seldom discovered at distances farther than about 0.75 AU, primarily because they are not easily discriminated from other asteroids by their motion at larger distances. The conical volume sampled at a limit of detection of 0.3 AU is 1.7×10^{-4} $(AU)^3$, which is 3.3×10^{-5} of the volume of a spherical shell around the Sun with inner and outer radii of 1.0 and 1.3 AU. In cases where the asteroid is fainter than H = 17.7, or where the threshold of detection is brighter than V = 16.5, the volume of the conical detection space for each field is correspondingly smaller. At a detection limit of 0.75 AU, the conical volume is 2.6×10^{-3} $(AU)^3$, or 1.4×10^{-4} of the volume of the detection shell extending to 1.75 AU from the Sun.

The differential probability, dp_H, for discovery of an asteroid of a given absolute magnitude H with a pair of photographs of a single field may be written as

$$dp_H = c\, f_H\, dN_H, \qquad (2)$$

where c is the fraction of detectable objects found under the actual conditions of search, f_H is the mean fraction of time that asteroids of a given H spend within the discovery volume, and dN_H is the differential number of asteroids at magnitude H. We have modeled the cumulative number, N_H, as a function of H by two sequential exponential functions, as described below and illustrated in Figure 1. The fraction f_H depends on the distances to which an asteroid of magnitude H may be detected (hence, on the mean volume sampled by individual search fields), and on the average time that Earth-crossing asteroids will spend in specific

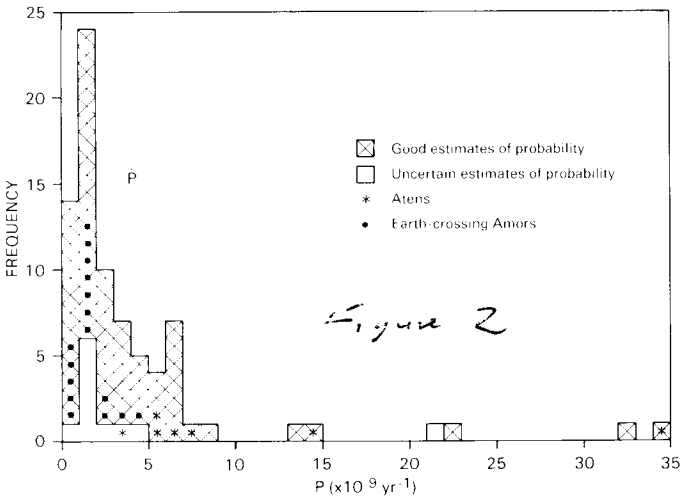

Figure 1. Magnitude-frequency distribution of Earth-crossing asteroids.

volumes of space. The mean volume depends on the distribution of α in our survey and the distribution of $f(\alpha)$ among the photometric types of Earth-crossing asteroids. We adopted a distribution of $f(\alpha)$ on the assumption that the *observed* distribution of photometric types among Earth crossers reported by McFadden and others (1989) is representative of the objects expected to be found in the detection volumes. This procedure should yield the correct estimate of the proportion of bright (S-type) and dark (C-type) asteroids in the Earth-crossing population, as discussed below, and of the total population.

The mean time spent by asteroids in the conical detection volumes is evaluated by means of Kepler's equation for the set of orbits of discovered Earth-crossing asteroids. This set is taken to be representative of the objects to be found in the detection volumes but not of the population of Earth crossers. Asteroids with relatively low aphelia (small semimajor axes and moderate eccentricities) have larger fractional dwell times in the detection region than asteroids with high aphelia. Also, each asteroid is restricted in its distribution within the detection shell about the Sun to a sector bounded by $\pm$ the inclination of the asteroid's orbit from the ecliptic. As our survey extends only to about 12° from the ecliptic at 1.3 AU from the Sun, for example, asteroids with orbital inclinations greater than 12° spend less time in the detection region and have lower probability of discovery than asteroids with lower inclination. While the *mean* dwell time should be correctly estimated from the orbits of the discovered asteroids, the distribution of the observed orbital elements is strongly biased with respect to that of the total population. In the limit where discoveries are made when the asteroids are close to Earth, the dwell times in the discovery volumes are approximately proportional to the probability of collision with Earth divided by the encounter velocity. The distributions of orbital elements for the population of Earth crossers can be roughly estimated from the observed distributions by weighting each observed element by the encounter velocity divided by the collision probability.

Integration of equation (2) yields the expression

$$p_H = c\,\bar{f}_H\,N_H, \tag{3}$$

where p_H is the cumulative probability of discovery with a single search field for asteroids brighter than H, and $\bar{f}_H$ is the mean fractional dwell time of asteroids in the conical detection volumes, evaluated over the range of magnitudes from that of the brightest Earth crosser to H. Because few Earth-crossing asteroids are actually discovered at distances much greater than about 0.75 AU, the numerical evaluation of $\bar{f}_H$ is insensitive to the precise functional dependence of N_H on H at magnitudes brighter than about H = 15.0.

The number, n_H, of asteroids brighter than H expected to be discovered by our survey is given by

$$n_H = p_H\,s(1\ b), \tag{4}$$

where s is the total number of fields photographed, and b is the overlapping fraction of the search fields. Combining equations (3) and (4), we have

$$N_H = \left(\frac{n_H}{s}\right)\left(\frac{1}{\bar{f}_H\,c(1-b)}\right). \tag{5}$$

Through September, 1989, the total number of fields, s, photographed in our survey was 4,175. The total conical volume sampled by these fields is equivalent to 14 percent of the volume of the detection shell to 1.3 AU, at the detection limit Δ = 0.3 AU, and to 59 percent of the detection shell to 1.75 AU at the detection limit Δ = 0.75 A.U. In these fields, 13 Earth-crossing asteroids brighter than H = 17.7 were discovered or independently found (Table 2), yielding a ratio of 3.1 Earth crossers with $H \leqslant 17.7$ per thousand fields. The photographic techniques and films used varied over the course of the survey, but most detections were made when the threshold of detection was close to V = 16.5 for fast-moving asteroids. This threshold is determined from the faintest objects found among more than 40 detected Earth-approaching asteroids and is adjusted for the length of the trailed image. The detection threshold for slow-moving asteroids is more than a magnitude fainter. Our estimate of $\bar{f}_H$ is 5.16×10^{-6}. The fraction of detectable objects found, c, is estimated from one documented case where a near-Earth asteroid was missed but discovered by others and from a small number of fast-moving asteroids that we detected but were unable to follow and for which no orbits are available. Discoveries can be missed when one or both images of the asteroid on the photographic pair are superimposed on images of stars. We estimate c = 0.9. The overlapping fraction, b, of the fields taken is 0.35. When these values are used in equation (5), the number of Earth-crossing asteroids brighter than H = 17.7 is found to be 1,030.

TABLE 2. EARTH-CROSSING ASTEROIDS BRIGHTER THAN H = 17.7 DETECTED IN THE PALOMAR ASTEROID AND COMET SURVEY, 1982 TO SEPTEMBER 1989

		H	Detection circumstances					
			Detection	Date	V	Δ (AU)	r (AU)	α (°)
Aten								
3554	Amun	15.94	Discovered	3/04/86	14.7	0.267	1.233	22.8
Apollos								
1620	Geographos	15.61	Detected	2/11/83	13.3	0.263	1.214	20.8
3671	Dionysius	17.0	Discovered	5/27/84	14.1	0.147	1.116	43.0
4183	1959 LM	14.6	Rediscovered	6/24/87	16.1	0.787	1.695	22.8
4341	1987 KF	15.5	Discovered	5/29/87	15.8	0.437	1.351	33.1
4450	1987 SY	17.7	Discovered	9/25/87	16.0	0.308	1.317	13.4
	1984 KB	16.4	Discovered	5/27/84	12.8	0.139	1.116	40.0
	1987 SB	15.5	Found	9/27/87	16.2	0.692	1.691	4.4
	1988 VP4	15.5	Discovered	11/04/88	16.9	0.746	1.642	22.3
	1989 FB	17.5	Discovered	3/31/89	15.8	0.298	1.289	11.6
Earth-crossing Amors								
1627	Ivar	13.24	Detected	4/13/85	14.1	0.640	1.431	37.9
3551	1983 RD	16.81	Found	9/07/83	13.2	0.098	1.097	22.3
	1986 DA	15.94	Found	2/05/86	15.4	0.398	1.374	11.0

Note: H is absolute V magnitude, V is apparent V magnitude, Δ is distance from Earth, r is distance from Sun, α is phase angle.
Discovered denotes discovered in this survey.
Detected indicates serendipitous detection of a known asteroid.
Rediscovered indicates second discovery of a lost asteroid.
Found indicates independent detection of an asteroid close to the time of its discovery by other observers.

One of the largest uncertainties in the estimate of the population lies in the small number of detected asteroids brighter than H = 17.7. The statistical uncertainty for 13 detected objects is ±28 percent (one standard deviation). Another substantial uncertainty, probably of comparable or greater magnitude, lies in the estimation of $\bar{f}_H$. The accuracy of this estimate depends on correctly assessing the threshold magnitudes of detection, on estimating the distribution of photometric functions for the asteroids residing in the detection volumes, and on the reliability of the inferred magnitude-frequency distribution in the range $15.0 \leqslant H \leqslant 17.7$. It should be noted that likely errors result in overestimation of $\bar{f}_H$ and, therefore, underestimation of the population. Adverse conditions of observing and imperfect focus shift the detection threshold for some of the fields photographed; correction for these effects can decrease the effective value of $\bar{f}_H$. Finally, there is uncertainty in our estimate of c, the fraction of detectable objects actually found. It is possible that our estimate of 0.9 is optimistic; more asteroids brighter than our detection threshold may have been missed than we are aware of. A lower value for c would also increase the estimate of the population. Taking the root of the sum of the squares of the estimated uncertainties, we suggest that the uncertainty to be assigned to our estimate of the population is about ±45 percent. The error is not strictly symmetrical; it is more likely that the population is larger than we have estimated than lower.

Estimated populations for each orbital type of Earth crosser can be obtained from the proportions of the discovered objects brighter than H = 17.7. Because the statistics of discoveries from our Palomar Asteroid and Comet Survey are so limited, it is more appropriate to utilize the entire set of discovered Earth crossers brighter than magnitude 17.7, as shown in Table 3. Dividing the number discovered in each orbital category by the estimated total fraction discovered (5.7 percent) yields estimates for the populations of Atens, Apollos, and Earth-crossing Amors uncorrected for observational selection effects. The uncorrected estimate for the cumulative number of Apollos plus Atens at H = 17.7 is 770 ± 340. This number is close to an estimate of 800 ± 300 derived from a total of nine asteroids discovered in a prior survey with the Palomar 46-cm Schmidt, conducted from 1973 through 1978, and in the Palomar National Geographic Sky Survey and Lick Observatory Proper Motion Survey, both of which were carried out between 1949 and 1956 (Helin and Shoemaker, 1979). The

TABLE 3. ESTIMATED POPULATIONS OF EARTH-CROSSING ASTEROIDS

	Number discovered (H <17.7)	Percent discovered	Uncorrected estimate of population (H <17.7)	Weighting factor	"Bias corrected" estimate of population (H <17.7)	Best estimate of population (H <17.7)
Atens	4	(5.7)	70 ± 40	0.24	20 ± 10	30 ± 20
Apollos	40	(5.7)	700 ± 300	0.85	590 ± 250	660 ± 280
Earth-crossing Amors	15	(5.7)	260 ± 130	1.62	420 ± 210	340 ± 170
Total Earth crossers	59	5.7	1,030 ± 470		1,030 ± 470	1,030 ± 470

Note: Percentages enclosed in parentheses indicate assumed values before bias correction. The weighting factors are proportional to the encounter velocity divided by the reciprocal of the mean probability of collision with Earth for each class of Earth-crossing asteroid.

methods of estimation, analogous to those used here, were very briefly described by Shoemaker and others (1976).

An approximate correction for observational selection effects can be obtained by weighting the observed numbers of Atens, Apollos, and Earth-crossing Amors by a factor proportional to the mean encounter velocity and to the reciprocal of the mean collision probability with Earth for each orbital class. This weighting scheme yields about the right ratio of Atens to Apollos but tends to overestimate the number of Amors, because of failure of the limiting approximation in the case of Amors. Hence, the numbers of Atens and Apollos are underestimated. Best estimates for the populations of Apollos and Earth-crossing Amors probably are about midway between the uncorrected and the "bias corrected" values (Table 3). Our best estimate of the combined number of Atens and Apollos at H = 17.7 is 690 ± 310. This number may be compared with a theoretically predicted steady-state population of 454 to 610 Atens and Apollos derived from collisional fragmentation of main-belt asteroids (Wetherill, 1988). Within the errors of estimation from observation and of theoretical calculation, these estimates can be considered to be in good agreement.

Present evidence suggests that the discovery of Earth-crossing asteroids is complete at H = 13.24, the magnitude of the brightest known object. This magnitude is close to the threshold for approximate completeness of discovery for asteroids orbiting near the inner edge of the main asteroid belt. Because the completeness of discovery declines rapidly for fainter objects, the magnitude-frequency distribution of the Earth-crossing population can only be inferred from indirect evidence. We have used two independent lines of evidence to evaluate the probable magnitude distribution: (1) observations of faint main belt asteroids, and (2) the size-frequency distribution of young craters on the Moon. Observations of faint main belt asteroids in a systematic survey by van Houten and others (1970) indicate that the cumulative frequency of faint asteroids, for various parts of the main belt, is approximately proportional to $e^{0.9H}$. Dohnanyi (1971) suggested that this distribution of magnitudes is consistent with a collisionally relaxed size distribution for small asteroids. If Earth-crossing asteroids are chiefly collision fragments derived from the main belt, then their magnitude distribution should also be consistent with that expected from collisional fragmentation and should resemble the distribution of small objects in the main belt. These expectations are supported by the observed size distribution of young lunar craters. The cumulative number, N_D, of craters of Copernican age (formed in roughly the last billion years) in the diameter range 10 to 60 km is very nearly proportional to D^{-2}, where D is crater diameter (Wilhelms, 1987). After corrections are made for different amounts of crater collapse for craters of different sizes and for crater scaling as a function of projectile size, it can be shown that the cumulative number of impacting bodies probably was also closely proportional to the inverse square of their diameters. The corresponding distribution of magnitudes, for bodies of about the same albedo, has the form

$$N_H = K\, e^{gH}, \tag{6}$$

where

$$g = \frac{-2}{5 \log_{10} e} = 0.9_2.$$

Substituting $N_H = 1030$ at H = 17.7, the value of the proportionality constant, K, of equation (6) is found to be 8.7×10^{-5}. As may be seen from Figure 1, a curve with this value of K and g = 0.92 does not pass through the point $N_H = 1$ at H = 13.24. Hence, this curve cannot represent the entire magnitude frequency distribution up to the brightest object. The cumulative frequency distribution evidently steepens as the brightest object is approached. For the magnitude distribution of the brightest Earth crossers, we have adopted a curve intercepting N = 1 at H = 13.24 with the form of equation (6) but with g = 2. The inferred steep curve for the bright objects clears, by a small margin, the observed frequency for discovered asteroids at about H = 14.2. This steep curve joins the distribution adopted for fainter asteroids at about H = 15.8; of course, the exact form of the frequency distribution near this junction or "knee" is conjectural. The steepening of the

frequency distribution at the bright end of the magnitude range is an expected consequence of the collisional origin of Earth-crossing asteroids, as will be explained below.

A check on the inferred magnitude-frequency distribution of the Earth-crossing asteroids is provided by the frequency with which Earth crossers have been accidently rediscovered (Table 4). Nine have been rediscovered or recovered without deliberate search. The probability of rediscovery is a strong function of absolute magnitude. Rediscovered asteroids are all brighter than H = 16.25; most are magnitude 15 or brighter. The brightest Earth crosser, (1627) Ivar, was discovered in 1929, then lost, rediscovered in 1957, and serendipitously recovered in 1985 with the Palomar 46-cm Schmidt. Another Earth-crossing asteroid as bright as or brighter than Ivar is unlikely to have escaped detection. Four out of 11 known objects in the magnitude range 13.0 to 14.9 have been accidentally rediscovered, which suggests that completeness of discovery to H = 14.9 is about 36 percent; the completeness indicated in Figure 1 is 36 percent. Four out of 21 known objects, or 19 percent, have been rediscovered in the magnitude range 15.0 to 15.9. This may be compared with the ratio of 12 percent for the number discovered to the population predicted in this range. Within the large uncertainty due to small statistics for rediscoveries, the two ratios are similar. One object out of 29 (3.4 percent) has been discovered in the magnitude range 16.0 to 17.7, as compared with a rediscovery rate of 3.5 percent predicted from Figure 1. The probability of rediscovery is also a function of orbital characteristics; the list of rediscovered objects includes the two brightest known Atens, members of the orbital class for which discovery is expected to be most complete.

TABLE 4. REDISCOVERIES OF EARTH-CROSSING ASTEROIDS

Range of magnitude (H)		H	Fraction rediscovered	
13.0–14.9	1627 Ivar	13.24	4/11	(36%)
	4179 1989 AC	14.2		
	3122 1981 ET3	14.3		
	4183 1959 LM	14.6		
15.0–15.9	3573 1986 TO	15.0	4/21	(19%)
	2201 Oljato	15.56		
	1620 Geographos	15.61		
	1863 Antinous	15.81		
16.0–17.7	2100 Ra-Shalom	16.21	1/29	(3%)

PROBABILITIES OF ASTEROID COLLISION WITH EARTH

Probabilities of collision of Earth-crossing asteroids with Earth can be calculated by means of a general approach first introduced by Öpik (1951). Near the time of orbit crossing, collision is possible when the orbit of the asteroid intersects the capture cross section of Earth. The collision probability depends on the fraction of time during which intersection occurs and on the frequency with which the asteroid is at the right orbital position for collision. In Öpik's original calculation of collision probabilities, he assumed the rate of advance of perihelion to be uniform and the semimajor axis, a, eccentricity, e, and inclination, i, of an asteroid's orbit to be constant during precession. Shoemaker and others (1979) replaced these assumptions with a more realistic formulation that uses the derivative with respect to time of the radius to the node, dr/dt, and estimated values of a, e, and i at the times of crossing. These terms may be found either from secular perturbation theory or from numerical integration of the motion of the asteroid.

Irregularities of the secular perturbations of asteroid orbits due to the eccentricities and inclinations of the perturbing planets cause dispersion in dr/dt and in the orbital elements e and i at times of Earth crossing. Moreover, because of the eccentricity and the variations in the elements of Earth's orbit, crossings occur over a range of nodal distance and over an increased range of dr/dr, e, and i of the asteroid orbits. To simplify calculation of the collision probability, we have selected representative values for the radius to the node at the time of crossing and for each crossing parameter.

In calculating collision probabilities for Atens and deep-crossing Apollos, the mean distance of Earth from the Sun (1 AU) has been taken as the representative crossing radius; representative crossing values of a, e, i, and dr/dt, for crossings at this distance, are listed in Table 1. The collision probability, designated Ps in Table 1, was determined from these parameters and from the precession period, Tc, by means of equations presented by Shoemaker and others (1979). Also shown are alternative solutions for the collision probability, designated Po, which are based on the listed crossing values of a, e, and i but were obtained from the simplified equations of Öpik (1951). Significant differences are found between Po and Ps for individual asteroids, but the differences tend to average out. In most cases, Öpik's equations lead to moderate overestimation of the collision probability.

For shallow-crossing Amors and Apollos, we adopted the mean aphelion distance of Earth, 1.028 AU, as the representative radius to the node at crossing; mean i when full crossing depth is reached was taken as the representative inclination. The eccentricity shown in Table 1 for each of these asteroids is the value obtained by setting the difference between the adopted aphelion distance of Earth and the perihelion distance of the asteroid equal to the crossing depth. Numerical experiments suggest that these crossing parameters may be used to obtain stable estimates of the collision probabilities. To obtain the values of Po listed in Table 1 for shallow crossers, the probabilities calculated from Öpik's equations were multiplied by the estimated fraction of the time that the eccentricity is sufficiently high to permit crossings.

Two distinct sets of the crossing parameters e, i, and dr/dt

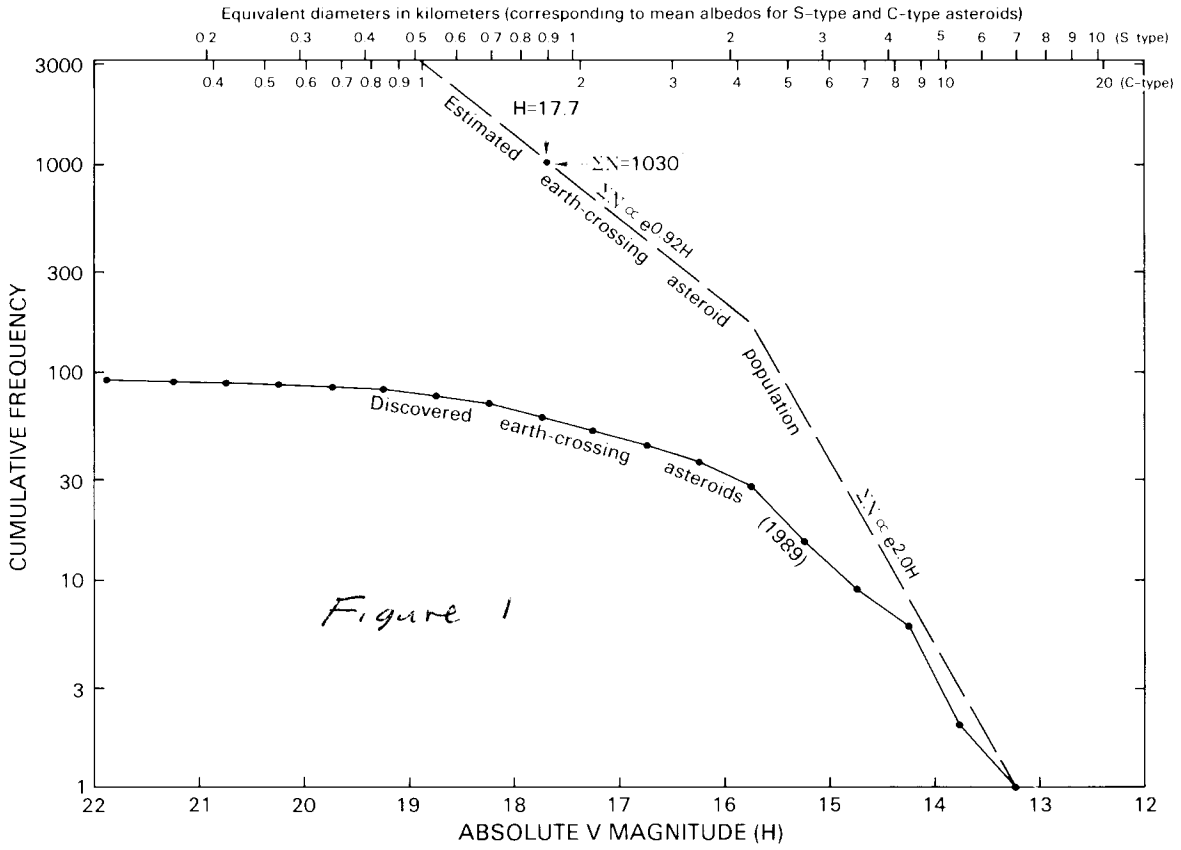

Figure 2. Frequency distribution of probabilities of collision with Earth for Earth-crossing asteroids.

are shown for several asteroids. These different sets arise in cases where large oscillations of e lead to twice the usual number of crossings during a precession cycle, or where the major axis does not precess in the usual manner but librates about a direction perpendicular to the line of the nodes. Asteroids having exceptionally high inclination exhibit these anomalous types of dynamical behavior. The values of Ps and Po shown for these asteroids are the sums of the probabilities for both conditions of crossing.

We have been unable to derive representative crossing parameters for a few Atens and Apollos, either because their orbits lie close to secular resonances or, in one instance, because the asteroid is a Jupiter crosser. In these cases, we adopted the present (osculating) elements as estimates of the crossing values so that we could obtain crude estimates of the collision probabilities from Öpik's equations.

Seven Earth-crossing asteroids librate around mean motion commensurable with the motion of Jupiter. Three are in the 3:1 commensurability (three revolutions of the asteroid for each revolution of Jupiter), three are in the 5:2 commensurability, and one is in the 2:1 commensurability (Table 1). The secular variations of the orbital elements of these asteroids are so irregular that we are unable to estimate representative collision parameters. Numerical integration suggests that the Amor asteroid (1915) Quetzalcoatl, for example, will become an extremely deep Earth crosser in 30,000 years, whereas the orbit of 1986 JK, which is presently an Earth crosser, will evolve to low eccentricity in 30,000 years, when 1986 JK will remain far from Earth (Hahn and Lagerkvist, 1988).

The frequency distribution of collision probabilities is illustrated in Figure 2. Values of Ps are used where available; Po is used for the remainder of the asteroids for which we were able to calculate a collision probability. The distribution is strongly skewed: though the mode is close to 1.5×10^{-9} yr^{-1}, half a dozen asteroids have collision probabilities substantially exceeding 10^{-8} yr^{-1}. Asteroids on small, low-inclination orbits that have relatively shallow overlap with Earth's orbit at the time of crossing have high probability of collision. The mean probability of collision is 10.7×10^{-9} yr^{-1} for Aten asteroids, 4.1×10^{-9} yr^{-1} for Apollos, and 1.4×10^{-9} yr^{-1} for Earth-crossing Amors. The distribution of the uncertain estimates of collision probability follows the distribution of the more reliable estimates rather closely. Hence, their inclusion does not significantly affect the calculated mean. The grand mean probability of collision obtained for all categories of Earth-crossing asteroids is 4.2×10^{-9} yr^{-1}. The uncertainty in this estimate probably is about ±40 percent; the chief source of uncertainty is the statistical error inherent in the small number of discovered asteroids with high collision probability. Although the discovered objects are not representative of the

Earth-crossing asteroid population, the mean collision probability of the discovered objects is a good estimate of the mean for the population, provided that the probability of discovery is approximately proportional to the probability of collision with Earth and inversely proportional to the encounter velocity. Weighting of each collision probability by its reciprocal does not change the mean and it eliminates any effect on the mean from weighting by the encounter velocities.

When we multiply the mean collision probability by the estimated population of Earth crossers at H = 17.7, the estimated present rate of collision for these objects is found to be $(4.3 \pm 2.6) \times 10^{-6}$ yr^{-1}. This estimate is about 30 percent higher than that reported by Shoemaker and others (1979), owing chiefly to the discovery in the last ten years of several asteroids having unusually high probabilities of collision. The colliding *flux* consists of about 75 percent Apollos, 10 percent Atens, and 15 percent Amors. In our model for the magnitude-frequency distribution, the collision rate of Earth crossers to H = 15.8 (roughly equivalent to S-type asteroids with diameters greater than 2 km) is about 7×10^{-7} yr^{-1}; the collision rate to H = 13 (asteroids roughly 9 km in diameter and larger) is about 3×10^{-9} yr^{-1}.

The present rate of production of craters by impact of Earth-crossing asteroids can be estimated from their collision rate with Earth, with the aid of (1) observations and inferences about the physical characteristics of Earth crossers, (2) the distribution of impact speeds (vi in Table 1), (3) the theoretical distribution of impact angles, and (4) crater-scaling theory. Among Earth crossers sufficiently well observed for photometric classification listed by McFadden and others (1989), 20 belong to relatively high albedo classes (S-, Q-, V-, or E-types), which we broadly group here as "S-type;" seven belong to low albedo classes (C-, F-, T-, or G-types), grouped here as "C-type"; and two have been categorized as M-type. Luu and Jewett (1989) pointed out a selection effect in the discovery of Earth-approaching asteroids that favors detection of S-types and discriminates against C-types. The effect is due to more rapid phase darkening of C-types than of S types (i.e., the phase function is steeper for low-albedo than for high-albedo asteroids). We have taken account of these differences in phase function in our evaluation of f_H, when estimating the population. From the actual distribution of the phase angles at the time of discovery of Earth crossers, we find that, on average, the absolute magnitude of C-type asteroids is about 0.16 magnitude brighter than that of S-types for a given apparent magnitude at the threshold of detection. For objects of the same absolute magnitude, the average limiting distance of detection is about 1.07 times greater for S-types than for C-types, and the average search volume is 1.24 times greater. The corrected ratio of S-types to C-types to a given absolute magnitude, therefore, is (20/1.24):7 or close to 2:1.

As estimated by Shoemaker and others (1979), an asteroid with the average albedo of S-types has a diameter of 0.89 km at V(1,0) = 18.0 (H = 17.7), and one with the average albedo of C-types a diameter of 1.73 km. Densities estimated on the basis of presumed meteorite analogues, with allowance made for bulking due to fragmentation, are 2.4 gm cm^{-3} for S-types and 1.7 gm cm^{-3} for C-types (Shoemaker and others, 1979). Hence, the estimated masses at H = 17.7 are 8.9×10^{14} gm for S-type and 4.6×10^{15} gm for C-type asteroids and the corresponding kinetic energies at the rms impact speed of 17.9 kms^{-1} obtained from Table 1 are 3.4×10^{7} and 1.76×10^{8} kilotons TNT equivalent, respectively (1 kiloton TNT = 4.185×10^{19} ergs).

The diameter of a crater produced by asteroid impact can be estimated from its kinetic energy by the empirical formula (Shoemaker and Wolfe, 1982)

$$D = 0.074\, c_f\, (g_e/g)^{1/6}\, (W\, \rho_a/\rho_t)^{1/3.4}, \qquad (7)$$

where D is the crater diameter in km, c_f is the crater collapse factor, nominally 1.3 for craters on Earth larger than 4-km diameter, g_e is the gravitational acceleration at the surface of the Earth, and g the acceleration at the surface of the body on which the crater is formed, W is the kinetic energy of the impacting body in kilotons TNT equivalent, ρ_a = 1.8 gm cm^{-3}, and ρ_t is the density of the target rock. A comparison of this simple energy scaling formula with the Holsapple-Schmidt scaling rules has been presented by Shoemaker (1983). The success of equation (7) in predicting crater diameters in the range 1 to 150 km has been demonstrated by a series of finite difference code calculations for cases of vertical impact (Roddy and others, 1980, 1987). A correction to the predicted crater diameter should be made for oblique impacts. We adopt the empirical formula of Gault (1973),

$$D_i = D\, (\sin i)^{2/3}, \qquad (8)$$

where D_i is the corrected diameter and i is the elevation angle of impact. At the modal elevation angle of 45° for an isotropic flux of impactors, the correction is 0.794. Applying equations (7) and (8) we find that a magnitude 17.7 S-type asteroid impacting at the root mean square (rms) speed 17.9 kms^{-1} and at 45° elevation angle to a terrestrial target with density 2.7 gm cm^{-3} produces a crater 11.1 km in diameter; a magnitude 17.7 C-type asteroid produces a crater 18.1 km in diameter.

A 10-km-diameter crater is produced by an S-type asteroid slightly fainter than H = 17.7. As the cumulative number of asteroids is proportional to the inverse square of their diameter, according to our model distribution, the cumulative number of craters varies with the inverse $(3.4/3) \times 2 = 2.27$ power of the crater diameter (for craters in the size range where the collapse factor remains constant). Hence, the cumulative number of craters at 10 km diameter is $(10/11.1)^{-2.27} = 1.27$ times higher than at 11.1 km diameter and $(10/18.1)^{-2.27} = 3.8$ times higher than at 18.1 km diameter. Taking two-thirds of the estimated flux colliding with Earth at H = 17.7 as S-type asteroids, impact of these bodies produces craters equal to or larger than 10 km diameter at the rate of $1.27 \times (2/3) \times 4.3 \times 10^{-6}$ yr^{-1} = 3.6×10^{-6} yr^{-1}; C-type asteroids, at one-third of the flux, produce 10 km and larger craters at the rate $3.8 \times (1/3) \times 4.3 \times 10^{-6}$ yr^{-1} = 5.4 ×

10^{-6} yr^{-1}. (For simplicity we apportioned part of the small flux of M-types to the S-type asteroid flux and part to the C-type). The total estimated cratering rate to 10-km diameter craters is $(9 \pm 5) \times 10^{-6}$ yr^{-1}, for the whole Earth, or $(1.8 \pm 1.0) \times 10^{-14}$km^{-2} yr^{-1} per unit area; 40 percent of the craters are produced by impact of S-type asteroids and 60 percent by C-type. This estimate of the cratering rate is 25 percent lower than that of Shoemaker (1983), owing to our slightly lower estimate of the rms impact speed, our somewhat lower estimate of the fraction of C-type asteroids, and our adoption here of the Gault formula for oblique impact.

Spectrophotometric data and infrared observations, obtained chiefly in the last decade, show that the large majority of well-observed Earth crossers are similar to asteroids found in the inner part of the main belt (McFadden and others, 1989). The combination of asteroid-asteroid collisions in the main belt, resonant perturbations of the orbits of collision fragments, and further perturbation of asteroid fragments by encounters with Mars appears adequate to replace losses of Earth-crossing asteroids due to collisions with planets as well as to ejection from the Solar System (Wetherill, 1988). Variations in the rate of delivery of collision fragments were studied by Shoemaker (1984), who found that the number of Earth crossers larger than 1-km diameter that are derived from main-belt asteroids probably has remained steady within about 5 percent through most of the last 3 billion years. However, population surges of about 25 percent above the mean level, which were due to breakup of main-belt asteroids on the order of 100 km in diameter, probably occurred at average intervals of about a half billion years. Durations of these surges above half maximum are estimated to be about 3×10^7 years. In addition to these stochastic fluctuations of the population, periodic modulation of the near-Earth asteroid flux has occurred at a frequency of 10^{-5} yr^{-1}, as a result of secular variation of the eccentricity of Earth's orbit. The amplitude of this latter modulation is estimated to be about ±5 percent from the mean flux.

The situation is somewhat different for the largest Earth crossers. Two-thirds of the production of asteroids 1 km in diameter and larger are estimated to be derived from the disruption of main belt precursors 2 to 10 km in diameter; only 15 percent of the small Earth crossers are derived from precursors larger than 50 km in diameter (Shoemaker, 1984). On the other hand, Earth crossers about 10 km in diameter are supplied chiefly by catastrophic breakup of main belt asteroids on the order of 30 to 100 km in diameter. As shown in Table 5, breakup of 50- to 100-km asteroids, which accounts for about half the production of 10 km and larger fragments, occurs at average intervals of about 6×10^7 to 3×10^8 years. About half these disruption events are likely to take place close enough to a resonance for fragments to be delivered to Earth-crossing orbits. When breakup of a large asteroid does occur near a resonance in the main belt, the number of Earth crossers brighter than H ≈14 may increase rather suddenly by an order of magnitude. As the typical dynamical lifetime of Earth-crossing asteroids is only about 3×10^7 years, the surge in the flux of large asteroids near Earth soon dies away. Most of the time there is a dearth of large (≥10 km diameter) Earth-crossing asteroids, because the characteristic time for their removal is about 4 to 20 times shorter than the mean time interval between main belt catastrophies that produce most of them.

TABLE 5. RATE OF COLLISIONAL DISRUPTION OF MAIN BELT ASTEROIDS*

Asteroid diameters	Disruption rate	Mean interval between disruptions	Total asteroids disrupted in 3 Gyr
≥1 km	4.4×10^{-3} yr^{-1}	2.3×10^3 yr	1.3×10^4
≥10 km	1.2×10^{-6} yr^{-1}	8.3×10^5 yr	3.6×10^3
≥30 km	6.3×10^{-8} yr^{-1}	1.6×10^7 yr	1.9×10^2
≥50 km	1.6×10^{-8} yr^{-1}	6.1×10^7 yr	49
≥100 km	3.2×10^{-9} yr^{-1}	3.1×10^8 yr	10
≥200 km	4.5×10^{-10} yr^{-1}	2.2×10^9 yr	1

*From Shoemaker, 1984.

There is about a 60 percent chance that a surge in the population of large Earth crossers reaching a peak of ten or more objects ≥10 km in diameter occurred during the Phanerozoic, according to the calculations by Shoemaker (1984). He noted that the exceptionally large (15 × 30 km) Amor asteroid Eros, which approaches Earth but is not presently Earth-crossing, is a likely example of a body produced by disruption of a ≥100 km precursor and stranded in a relatively long-lived orbit by encounters with Mars. The existence of Eros, whose dynamical lifetime is less than the span of the Phanerozoic (Wetherill and Shoemaker, 1982), suggests that a disruption of a major main belt asteroid and an accompanying surge in the flux of large Earth crossers did, in fact, occur in the last 6×10^8 years.

In addition to collisional fragments derived from the main asteroid belt, extinct or inactive comet nuclei probably are represented among the Earth-crossing asteroids (Weissman and others, 1989). Likely or possible extinct comets among the objects listed in Table 1 are 5025 P-L (chaotic, Jupiter-crossing orbit; associated meteor stream, Olsson-Steel, 1988); 1986 JK (radar properties strongly suggestive of a cometary body, Ostro and others, 1989; possible associated meteor stream, Olsson-Steel, 1988); (2101) Adonis (radar properties resembling those of known icy bodies, Ostro, 1985, 1987; associated meteor stream, Olsson-Steel, 1988); (2201) Oljato (peculiar spectral reflectance, McFadden and others, 1984; apparently associated disturbance of the solar wind, Russell and others, 1984; chaotic orbital evolution, Hahn and Lagerkvist, 1988; associated meteor stream, Olsson-Steel, 1988); and (3200) Phaethon (probable source of the very strong Geminid meteor stream). Other Earth-crossing asteroids with possible associated meteor streams include (1566) Icarus, 1984 KB, (2212) Hephaistos, (4197) 1982 TA, 1937 UB, (1962) Apollo, 1983 LC, 1987 SY, and 6344 P-L (Olsson-Steel and Lindblad, 1987; and Olsson-Steel, 1988). An associated meteor stream is not, by itself, a criterion of cometary origin,

because fine debris ejected by impacts on asteroids, as well as particles from comets, can be expected to form meteor streams. Apollo asteroid 1984 KB has a reflection spectrum and albedo closely similar to that of typical S-type asteroids in the main belt (Bell and others, 1988); this asteroid is also the probable source of a moderately well-defined stream of radar meteors. We regard the latter as a likely example of an impact dust stream derived from a rocky object of main-belt origin.

It is difficult to assess the fraction of Earth-crossing asteroids of cometary origin. Physical and dynamical evolution of very short period comets, such as Comet Enke, conceivably could account for as many as half the Earth crossers brighter than a given absolute magnitude (cf., Wetherill, 1988). The spectrophotometric similarity of most Earth crossers to asteroids in the inner part of the main belt, on the other hand, suggests that only a small fraction consists of extinct comets. Circumstantial evidence indicates that many or most extinct comets are dark, reddish (D-type) bodies (Hartmann and others, 1987); no D-type asteroids have been recognized along the Earth crossers, but repeated close passage by the Sun might have altered their surface optical properties (cf., Shoemaker and Helin, 1978; Weissman and others, 1989).

FLUX AND COLLISION RATE OF ACTIVE COMETS

The number of active, Earth-crossing comets discovered so far is about four times greater than the number of known Earth-crossing asteroids, but reliable data on the sizes of comet nuclei are sparse. Still less is known about the densities of comet nuclei. As a consequence of these uncertainties there has been a wide divergence of opinion about the rate of production of craters by comet impact (cf., Shoemaker and Wolfe, 1982; Weissman, 1982, and this volume; Olsson-Steel, 1987; Bailey and Stagg, 1988).

The basic difficulty in estimating the sizes of comet nuclei is that the solid nucleus is very rarely observed. Most observations of comets are made when they are relatively close to the Sun and the nucleus is shrouded in an atmosphere of gas and dust, called the coma. Even the existence of a solid nucleus was doubted by many investigators until about 1950. Most attempts to evaluate cratering rates by comet impact have utilized tabulated estimates of the absolute total magnitude (the calculated total magnitude at $\Delta = 1$, $r = 1$) of observed comets. Various theoretical arguments were invoked to deduce the size of the nucleus from the absolute total magnitude, which is utterly dominated by light from the coma. A review and update of this approach is provided in the accompanying paper by Weissman (this volume).

Here, we briefly review an alternative approach to the comet cratering rate based on an entirely different set of observations. Photographic observations of comets taken at times when the comets were relatively far from the Sun and least active, together with the record of comet discoveries, were used by Shoemaker and Wolfe (1982) to estimate the near-Earth flux and magnitude-frequency distribution of comet nuclei. The observations used were a set of photographic *nuclear* magnitudes obtained by Elizabeth Roemer and her colleagues at the Flagstaff Station of the U.S. Naval Observatory from April, 1957 through October, 1965. Magnitudes were obtained for 42 short-period comets and 25 long-period comets. The photographic plates were exposed specifically to determine accurate positions of the comet nuclei and probably represent the most homogeneous data set of this kind. In most cases, no coma was detected on Roemer's photographic plates when a comet was at the greatest distance that she could follow it. Nevertheless, Shoemaker and Wolfe found that even the most distant observations generally were contaminated by light from the unresolved coma. They estimated that, on average, only ~12 percent of the light recorded in these most distant observations was reflected from the solid surface of the nucleus. After correcting the photographic observations by magnitude 2.3 for the presence of unresolved coma, they estimated the present rate of collision with Earth of comet nuclei brighter than absolute B magnitude 18 to be about 10^{-7} yr^{-1}. The near-Earth flux is dominated by long-period comets; the contribution of short-period comets is neglected in this estimate. The mean probability of collision of long-period comets with Earth was obtained by means of Öpik's equations from about 400 published orbits. By far the greatest uncertainty in the estimate of the collision rate lies in the correction for coma. The error could be a factor of 2 or greater.

The cumulative frequency of comet nuclei was estimated from Roemer's observations to be proportional to $e^{0.91M}$, where M is the estimated absolute B magnitude of the inactive comet nucleus. In contrast to that of Earth-crossing asteroids, this distribution appears to extend to the brightest observed objects. Strong independent evidence for this approximate magnitude distribution of the nuclei was found from the size-distribution of ray craters on Ganymede, the largest satellite of Jupiter (Passey and Shoemaker, 1982), and from the size distribution of craters found on the grooved terrain of that satellite (Shoemaker and others, 1982). Estimates of the cratering rate by Shoemaker and Wolfe (1982) suggest that all but about 1 percent of these craters have been formed by a combination of active and extinct comets.

Several lines of evidence indicate that the albedos of comet nuclei generally are very low (e.g., A'Hearn, 1988). From the limited evidence available at the time, Shoemaker and Wolfe (1982) inferred that the average geometric albedo of comet nuclei in the B band is 0.03. This inference has been basically confirmed by spacecraft images of the nucleus of periodic Comet Halley (Keller and others, 1986; Sagdeev and others, 1986), radar and infrared observations of Comet IRAS-Iraki-Alcock (Sekanina, 1988), and infrared observations of the very weakly active periodic comets Arend-Rigaux and Neujmin 1 (Veeder and others, 1987; Campins and others, 1987; Millis and others, 1988). At an albedo of 0.03, Shoemaker and Wolfe calculated diameters for comet nuclei of 2.5 km, at absolute B magnitude 18, and 10 km at magnitude 15.

An interesting observational check on the flux of large comets has been provided by the close approach to Earth in 1983

of Comet IRAS-Araki-Alcock (1983 VIII). On the basis of the magnitude-frequency distribution found by Shoemaker and Wolfe, the rate of collision with Earth of comet nuclei 10 km in diameter and larger is about 10^{-8} yr^{-1} at the present comet flux; the corresponding mean rate at which these objects pass the Earth within a distance of 4.67 million km (0.0312 AU), the miss distance of IRAS-Araki-Alcock, is about once per 200 years. The geometric mean diameter of the elongate nucleus of IRAS-Araki-Alcock, determined from radar and infrared observations, is 9.3 km (Sekanina, 1988). This comet made the closest known approach of a cometary body to Earth since the apparition of Comet Lexell in 1770, 213 years earlier (Sekanina and Yeomans, 1984). Comparably near passes appear to have been made by comets in 1366 and 1491 (Sekanina and Yeomans, 1984); hence the mean interval between these close passes is very nearly 200 years. We do not know the nucleus sizes of these Earth-approaching comets seen prior to the present century, but our estimate of the flux suggests that they are all about the size of IRAS-Araki-Alcock or larger. If our estimate of the flux were too high, say by much more than a factor of 2, then the observed near pass of a comet the size of IRAS-Araki-Alcock in the present century would have to be considered an unlikely statistical fluke.

The most difficult step in estimating the cratering rate by comet impact is to obtain reliable estimates of the mean density of comet nuclei. Comets are composed chiefly of H_2O ice, a mixture of silicates, and complex polymerized organic compounds. Estimates of the density of the nucleus of comet Halley, the best-observed comet, span the range from about 0.2 gm cm^{-3} to more than 1.5 gm cm^{-3} (see Weissman, this volume). We regard estimates at the lower end of this range as physically implausible, as they imply unrealistic values of porosity.

Perhaps the best estimate of the mean grain density of long-period comets can be made from the bulk density of Triton and Pluto, two large objects that probably accreted in the region where most long-period comets were formed. On the assumption that Triton is differentiated, the silicate mass fraction is found to be 0.7, and the uncompressed density is in the range 1.8 to 2.0 gm cm^{-3}; a similar result is obtained for Pluto (Smith and others, 1989). The largest satellites of Uranus have bulk densities of 1.5 to 1.6 gm cm^{-3} (Smith and others, 1986) and inferred silicate mass fractions of about 0.6. The magnitude and size distributions of comet nuclei derived by Shoemaker and Wolfe are closely similar to those of main belt asteroids, which suggests that comets are collisionally evolved. Furthermore, studies of the scattering of Uranus-Neptune planetesimals to form the Oort comet cloud (Shoemaker and Wolfe, 1984) suggest that the original total mass of planetesimals was very large (i.e., several hundred Earth masses) and that most long-period comets are fragments or assemblages of fragments produced by mutual collision among the planetesimals. If we take 1.7 gm cm^{-3} as a mean estimate of the grain density and allow about 30 percent porosity as a typical value for bulking due to fragmentation in a low gravitational field, we obtain a predicted mean bulk density of about 1.2 gm cm^{-3} for comets derived from Uranus-Neptune planetesimals. This is identical with the density adopted by Shoemaker and Wolfe (1982) on the grounds of a different set of arguments. If most comets are fragments or aggregates of fragments derived from larger bodies, the precursor bodies may have partly differentiated; hence there may be a large diversity in composition and density among the comets.

In situ mass spectrometric observations of the coma of Halley (Kissel and others, 1986a, 1988b) revealed that much of the dust previously supposed to be silicate grains actually consists of a complex organic mixture composed of C, H, O, and N (so-called CHON particles). Thus the silicate mass fraction in Halley may be much lower than 0.6 to 0.7. This may indicate that Halley was derived from a different region than most long-period comets, perhaps the hypothesized trans-Neptunian belt of comets (Duncan and others, 1988) commonly referred to as the Kuiper belt. Alternatively, Halley may be a fragment of a differentiated planetesimal precursor. If we take the mean grain density of all constituents of a comet equal to the density of ice I at very low temperature (0.93 gm cm^{-3}) and assume a porosity of 50 percent as a physically realistic upper limit, we obtain a density of about 0.5 gm cm^{-3} as a lower limiting density for comet nuclei.

At the rms impact speed of 57.7 km s^{-1}, weighted by probability of collision, found for long-period comets and a typical angle of impact of 45°, B-magnitude 18 comet nuclei are estimated from equations (7) and (8) to produce craters 40 to 50 km in diameter, if their densities are in the range of 0.5 to 1.2 gm cm^{-3}. Craters of this size are comparable with those produced by average S-type asteroids of absolute V magnitude 14.2 to 14.8 (diameters of 3.4 to 4.6 km) impacting at the rms speed of 17.9 km s^{-1} of Earth-crossing asteroids. A 10-km-diameter comet nucleus with a density of about 1 gm cm^{-3} produces a crater about 150 km in diameter.

The flux of long-period comets almost certainly has been highly variable over late geologic time, owing chiefly to the nearly random perturbation of the Oort comet cloud by stars passing in the solar neighborhood. Monte Carlo studies (Heisler and others, 1987) suggest that surges in the near-Earth flux from three to more than 30 times the mean background flux of comets occurred at typical intervals of a few tens of millions of years. About half the comet impacts may have occurred during these surges or comet showers. It is not known from direct observations of comets whether the present flux lies close to the mean background flux of comets or whether it might represent a weak shower. The record of terrestrial impact glass and impact craters suggests that a mild comet shower may have occurred about 35 m.y. ago and that a very weak shower may have peaked about 1 m.y. ago (Shoemaker and Wolfe, 1986).

On the basis of bounds on the total production of large craters set by the Copernican crater record of the Moon (Wilhelms, 1987), we suggest that the present comet flux is not less than twice the mean background comet flux of the last billion years and might be roughly equal to the mean comet flux, including the contribution from showers. Because the present number of Earth-crossing asteroids drops so steeply for asteroids larger than

TABLE 6. ESTIMATED PRODUCTION OF CRATERS BY ASTEROID AND COMET IMPACT ON EARTH DURING THE LAST 100 MILLION YEARS

	Crater diameters (km)						
	>10	>20	>30	>50	>60	>100	>150
Asteroid impacts	910	190	58	8	3.2	0.3	0
Comet impacts	(280)	60	24	8	5.0	1.6	1
Total production	910	250	82	16	8	2	1

Note: Production of comet-impact craters smaller than about 20 km in diameter probably has been suppressed by breakup of the comet nuclei during passage through the atmosphere.

about 2 km in diameter (Fig. 2), it is possible that most observed Copernican craters larger than 60 km in diameter, such as Copernicus and Tycho, resulted from comet impact. If so, the Copernican craters larger than 60 km may give us an estimate of the integrated production of large, comet-impact craters over the last billion years and the mean comet flux during this interval. (Because gravity at the lunar surface is low, the rate of large-crater production by comet impact on the Moon is estimated to be about 1.6 times the rate on Earth; Shoemaker and Wolfe, 1987.) If during the last billion years there were several surges in the flux of large Earth-crossing asteroids, on the other hand, then most large Copernican craters may have been formed by asteroid impact. In this case, the present comet flux may be several times higher than the mean comet flux over the last billion years (i.e., the present flux corresponds to a mild comet shower).

CRATER PRODUCTION ON EARTH IN THE LAST 100 m.y.

Our best estimate of the production of impact craters on Earth over the last 100 m.y. is given in Table 6. In calculating the production of craters by comet impact, we assumed a mean density of 1.2 gm cm^{-3} for comet nuclei. To obtain the approximate number of craters expected to have formed on the continents, the figures in Table 6 should be divided by 3. The uncertainty attached to each of the figures in this table is at least a factor of 2. Our estimated production by asteroid impact of craters equal to and larger than 10 km in diameter is slightly greater than predicted from theory by Wetherill (1989) for the combined flux of Earth-crossing asteroids of cometary origin and of main-belt asteroidal origin. Production of craters smaller than 20 km in diameter by impact either of active or extinct comets probably has been suppressed by atmospheric breakup of comet nuclei (Melosh, 1981). Impact of active comets probably accounts for no more than half the Phanerozoic impact craters larger than 20 km in diameter. Large craters that may have been associated with mass extinctions in the last 100 m.y., on the other hand, are more likely to have been formed by comets than by asteroids.

The estimated total production of craters larger than 20 km in diameter is $(4.9 \pm 2.9) \times 10^{-15}$ km^{-2} yr^{-1}, which is quite consistent with the rate of $(5.4 \pm 2.7) \times 10^{-15}$ km^{-2} yr^{-1} estimated by Grieve (1984) from the geologic record of impact for the last 120 m.y. However, the corresponding number of lunar craters larger than 30 km in diameter expected to have been produced from the beginning of the Eratosthenian Period (3.3 billion years ago) is about twice the number of Copernican and Eratosthenian craters mapped by Wilhelms (1987). Although this difference is within the possible errors of estimation, we repeat the observation (Shoemaker and others, 1979; Grieve, 1984) that the mean cratering rate may have increased in late geologic time. An increase by as much as a factor of 2 could be most readily explained by an increase in the mean comet flux, but only if more than half the production of craters >30 km in diameter during the last 100 m.y. is due to comet impact.

Long-term changes in the average near-Earth comet-flux almost certainly have occurred as a consequence of changes in amplitude of the oscillation of the Sun normal to the galactic plane (z-oscillation). These changes are the result of encounters of the Sun with stars and molecular clouds. It is of interest that the present amplitude of the z-oscillation of the Sun is much less than the average amplitude for stars similar to the Sun. A decrease in amplitude of the z-oscillation late in geologic time would have led to an increase in the flux of long-period comets. Because the mean density of stars and other massive objects that perturb the Oort comet cloud is highest near the galactic plane, the Sun will spend more time in the region of high density of perturbing bodies when the z-oscillation is reduced. A large reduction of z-oscillation could have increased the average flux of comets near Earth by a factor of about 2.

EPILOGUE

After the calculations and first draft of this paper were prepared, five new Earth-crossing asteroids (1989 UP, 1989 UQ, 1989 UR, 1989 VA, and 1989 VB) were discovered during a single dark-of-the-moon observing period in late October and

early November 1989. Each asteroid was discovered with a different telescope at four different observatories on the Côte d'Azur, France, and at Kitt Peak, Arizona; Palomar, California; and Siding Spring, Australia. Two of the new objects are Aten asteroids, which bring the total of discovered Atens to nine. One of these (1989 VA) is brighter than H = 17.7; its discovery raises our estimate of the population of Atens at H = 17.7 by 25 percent to 40± 20. The spurt of discovery late in the year increased the rate to 13 Earth crossers per year in 1989, with two dark runs left to go. This high discovery rate reaffirms one of the basic observations of this report: Earth resides in an asteroid swarm.

ACKNOWLEDGMENTS

This work was supported in part by NASA funds transferred to the U.S. Geological Survey. We are deeply indebted to J. G. Williams, who generously provided us with a copy of his program to calculate crossing depths and the secular perturbations of asteroids. E. Bowell provided us with improved estimates of detection parameters, based on up to date orbits. P. Weissman and L. A. McFadden gave helpful reviews of an early draft of this paper. We thank Palomar Observatory for extensive observing time granted on the 46-cm Schmidt telescope.

REFERENCES CITED

A'Hearn, M. F., 1988, Observations of cometary nuclei: Annual Review of Earth and Planetary Sciences, v. 16, p. 273–293.

Bailey, M. E., and Stagg, C. R., 1988, Cratering constraints on the inner Oort cloud; Steady state models: Monthly Notices of the Royal Astronomical Society, v. 235, p. 1–35.

Batrakov, Yu. V. (editor-in-chief), 1987, Ephemerides of the minor planets for 1988: Leningrad, Institute of Theoretical Astronomy, 366 p. (in Russian and English)

Bell, J. F., Brown, R. H., and Hawke, B. R., 1988, Composition and size of Apollo asteroid 1984 KB: Icarus, v. 73, p. 482–486.

Bowell, E., Gehrels, T., and Zellner, B., 1979, Magnitudes, colors, types, and adopted diameters of the asteroids, *in* Gehrels, T., ed., Asteroids: Tucson, University of Arizona Press, p. 1108–1129.

Campins, H., A'Hearn, M. F., and McFadden, L. F., 1987, The bare nucleus of Comet Neujmin 1: Astrophysical Journal, v. 316, p. 847–857.

Dohnanyi, J. S., 1971, Fragmentation and distribution of asteroids, *in* Gehrels, T., ed., Physical studies of minor planets: National Aeronautics and Space Administration Special Paper 267, p. 263–292.

Duncan, M., Quinn, T., and Tremaine, S., 1988, The origin of short-period comets: Astrophysical Journal Letters, v. 328, p. L69–L73.

Gault, D. E., 1973, Displaced mass, depth, diameter, and effects of oblique trajectories for impact craters formed in dense crystalline rocks: The Moon, v. 6, p. 32–44.

Grieve, R.A.F., 1984, The impact cratering rate in recent time, *in* Proceedings, 14th Lunar and Planetary Science Conference: Journal of Geophysical Research, v. 89, p. B403–B408.

Hahn, G., and Lagerkvist, C.-I., 1988, Orbital evolution studies of planet-crossing asteroids, *in* Hahn, G., Physical and dynamical studies of planet-crossing asteroids [Ph.D. thesis]: Uppsala, Sweden, Uppsala University, 18 p.

Hartmann, W. K., Tholen, D. J., and Cruikshank, D. P., 1987, The relationship of active comets, "extinct" comets, and dark asteroids: Icarus, v. 69, p. 33–50.

Heisler, J., Tremaine, S., and Alcock, C., 1987, The frequency and intensity of comet showers from the Oort Cloud: Icarus, v. 70, p. 264–288.

Helin, E. F., and Shoemaker, E. M., 1979, Palomar planet-crossing asteroid survey 1973–1978: Icarus, v. 40, p. 321–328.

Keller, H. U., and 17 others, 1986, First Halley multicolour camera imaging results from Giotto: Nature, v. 321, p. 320–326.

Kissel, J., and 22 others, 1986a, Composition of comet Halley dust particles from Vega observations: Nature, v. 321, p. 280–282.

Kissel, J., and 18 others, 1986b, Composition of comet Halley dust particles from Giotto observations: Nature, v. 321, p. 336–337.

Luu, J., and Jewitt, D., 1989, On the relative numbers of C types and S types among near-earth asteroids: Astronomical Journal, v. 98, p. 1905–1911.

McFadden, L. A., Gaffey, M. J., and McCord, T. B., 1984, Mineralogical-petrological characterization of near-earth asteroids: Icarus, v. 59, p. 25–40.

McFadden, L. A., Tholen, D. J., and Veeder, G. J., 1989, Physical properties of Aten, Apollo, and Amor asteroids, *in* Binzel, R. P., Gehrels, T., and Matthews, M. S., eds., Asteroids II: Tucson, University of Arizona Press, p. 442–467.

Melosh, H. J., 1981, Atmospheric breakup of terrestrial impactors, *in* Merrill, R. B., and Schultz, P. H., eds., Proceedings of the Conference on Multi-ring Basins; Formation and Evolution: New York, Pergamon Press, p. 29–35.

Millis, R. L., A'Hearn, M. F., and Campins, H., 1988, An investigation of the nucleus and coma of Comet P/Arend-Rigaux: Astrophysical Journal, v. 324, p. 1194–1209.

Olsson-Steel, D. I., 1987, Collisions in the solar system; 4, Cometary impacts upon the planets: Monthly Notes of the Royal Astronomical Society, v. 227, p. 501–524.

——, 1988, Identification of meteoroid streams from Apollo asteroids in the Adelaide radar orbit surveys: Icarus, v. 75, p. 64–96.

Olsson-Steel, D. I., and Lindblad, B. S., 1987, 1987 SY: International Astronomical Union Circular 4472.

Öpik, E. J., 1951, Collision probabilities with the planets and distribution of interplanetary matter: Proceedings of the Royal Irish Academy, v. 54A, p. 165–199.

——, 1987, Planetary radar astronomy: Encyclopedia of Physical Science and Technology, v. 10, p. 611–634.

Ostro, S. J., 1985, Radar observations of asteroids and comets: Publications of the Astronomical Society of the Pacific, v. 97, p. 877–884.

Ostro, S. J., and 5 others, 1989, Radar observations of Asteroid 1986 JK: Icarus, v. 78, p. 382–394.

Passey, Q. R., and Shoemaker, E. M., 1982, Craters and basins on Ganymede and Callisto; Morphological indicators of crustal evolution, *in* Morrison, D., ed., The satellites of Jupiter: Tucson, University of Arizona Press, p. 379–434.

Roddy, D. J., Schuster, S. J., Kreyenhagen, K. N., and Orphal, D. L., 1980, Computer code simulations of the formation of Meteor Crater, Arizona; Calculations MC-1 and MC-2: Proceedings, 11th Lunar and Planetary Science Conference, Houston, Texas, Lunar and Planetary Institute, p. 2275–2308.

Roddy, D. J., and 5 others, 1987, Computer simulations of large asteroid impacts into oceanic and continental sites; Preliminary results on atmospheric, cratering, and ejecta dynamics: International Journal of Impact Engineering, v. 5, p. 525–541.

Russell, C. T., Aroian, R., Arghavania, M., and Nock, K., 1984, Interplanetary magnetic field enhancements and their association with asteroid 2201 Oljato: Science, v. 226, p. 43–45.

Sagdeev, R. Z., and 37 others, 1986, Television observations of comet Halley from Vega spacecraft: Nature, v. 321, p. 262–266.

Sekanina, Z., 1988, Nucleus of Comet IRAS-Araki-Alcock (1983 VII): Astronomical Journal, v. 95, p. 1876–1894.

Sekanina, Z., and Yeomans, D. K., 1984, Close encounters and collisions of comets with the Earth: Astronomical Journal, v. 89, p. 154–161.

Shoemaker, E. M., 1983, Asteroid and comet bombardment of the Earth: Annual Review of Earth and Planetary Sciences, v. 11, p. 461–494.

—— , 1984, Large body impacts through geologic time, *in* Holland, H. D., and Trendall, A. F., eds., Patterns of change in Earth evolution: Dahlem Konferenzen, F.R.G., Springer-Verlag, p. 15–40.

Shoemaker, E. M., and Helin, E. F., 1978, Earth-approaching asteroids; Populations, origin, and compositional types, *in* Morrison, D., and Wells, W. C., eds., Asteroids; An exploration assessment: NASA Conference Publication 2053, p. 161–176.

Shoemaker, C. S., and Shoemaker, E. M., 1988, The Palomar asteroid and comet survey (PACS), 1982–1987 [extended abs.], *in* 19th Lunar and Planetary Science Conference: Houston, Texas, Lunar and Planetary Institute, p. 1077–1078.

Shoemaker, E. M., and Wolfe, R. F., 1982, Cratering time scales for the Galilean satellites of Jupiter, *in* Morrison, D., ed., The satellites of Jupiter: Tucson, University of Arizona Press, p. 277–339.

—— , 1984, Evolution of the Uranus–Neptune planetesimal swarm [extended abs.], *in* 15th Lunar and Planetary Science Conference: Houston, Texas, Lunar and Planetary Institute, p. 780–781.

—— , 1986, Mass extinctions, crater ages, and comet showers, *in* Smoluchowski, R., Bahcall, J. N., and Matthews, M., eds., The galaxy and the solar system: Tucson, University of Arizona Press, p. 338–386.

—— , 1987, Crater production on Venus and Earth by asteroid and comet impact [extended abs.], *in* 18th Lunar and Planetary Science Conference, Part 3: Houston, Texas, Lunar and Planetary Institute, p. 918–919.

Shoemaker, E. M., Helin, E. F., and Gillett, S. L., 1976, Populations of planet-crossing asteroids: Geologica Romana, v. 15, p. 487–489.

Shoemaker, E. M., Williams, J. G., Helin, E. F., and Wolfe, R. F., 1979, Earth-crossing asteroids; Orbital classes, collision rates with Earth, and origin, *in* Gehrels, T., ed., Asteroids: Tucson, University of Arizona Press, p. 253–282.

Shoemaker, E. M., Lucchita, B. K., Plescia, J. B., Squyres, S. W., and Wilhelms, D. E., 1982, Geology of Ganymede, *in* Morrison, D., ed., The satellites of Jupiter: Tucson, University of Arizona Press, p. 435–520.

Smith, B. A., and 39 others, 1986, Voyager 2 in the Uraniam system; Imaging science results: Science, v. 233, p. 43–64.

Smith, B. A., and 63 others, 1989, Voyager 2 at Neptune; Imaging science results: Science, v. 246, p. 1422–1449.

van Houten, C. J., van Houten-Groenveld, I., Herget, P., and Gehrels, T., 1970, The Palomar–Leiden survey of faint minor planets: Astronomy and Astrophysics Supplement, v. 2, p. 339–448.

Veeder, G. J., Hanner, M. S., and Tholen, D. J., 1987, The nucleus of Comet P/Arend-Rigaux: Astronomical Journal, v. 94, p. 169–173.

Veeder, G. J., and 5 others, 1989, Radiometry of near-Earth asteroids: Astronomical Journal, v. 97, p. 1211–1219.

Weissman, P. R., 1982, Terrestrial impact rates for long- and short-period comets, *in* Silver, L. T., and Schultz, P. H., eds., Geological implications of impacts of large asteroids and comets on the Earth: Geological Society of America Special Paper 190, p. 15–24.

Weissman, P. R., A'Hearn, M. F., McFadden, L. A., and Rickman, H., 1989, Evolution of comets into asteroids, *in* Binzel, R. P., Gehrels, T., and Matthews, M. S., eds., Asteroids II: Tucson, University of Arizona Press, p. 880–920.

Wetherill, G. W., 1988, Where do the Apollo objects come from?: Icarus, v. 76, p. 1–18.

—— , 1989, Cratering of the terrestrial planets by Apollo objects: Meteoritics, v. 24, p. 15–22.

Wetherill, G. W., and Shoemaker, E. M., 1982, Collision of astronomically observable bodies with the Earth, *in* Silver, L. T., and Schultz, T. H., eds., Geological implications of impacts of large asteroids and comets on the Earth: Geological Society of America Special Paper 190, p. 1–13.

Wilhelms, D. E., 1987, The geologic history of the Moon: U.S. Geological Survey Professional Paper 1348, 302 p.

Williams, J. G., 1969, Secular perturbations in the solar system [Ph.D. thesis]: University of California at Los Angeles, 270 p.

MANUSCRIPT ACCEPTED BY THE SOCIETY JUNE 19, 1990